

Wavefield extrapolation by nonstationary phase shift

Gary F. Margrave* and Robert J. Ferguson*

ABSTRACT

The phase-shift method of wavefield extrapolation applies a phase shift in the Fourier domain to deduce a scalar wavefield at one depth level given its value at another. The phase-shift operator varies with frequency and wavenumber, and assumes constant velocity across the extrapolation step. We use nonstationary filter theory to generalize this method to nonstationary phase shift (NSPS), which allows the phase shift to vary laterally depending upon the local propagation velocity. For comparison, we derive an analytic form for the popular phase shift plus interpolation (PSPI) method in the limit of an exhaustive set of reference velocities. NSPS and this limiting form of PSPI can be written as generalized Fourier integrals which reduce to ordinary phase shift in the constant velocity limit. In the (x, ω) domain, these processes are the transpose of each other; however, only NSPS has the physical interpretation of forming the scaled, linear superposition of laterally-variable impulse responses (i.e., Huygen's wavelets).

The difference between NSPS and PSPI is clear when they are compared in the case of a piecewise constant velocity variation. Define a set of windows such that the j th window is unity when the propagation velocity

is the j th distinct velocity and is zero otherwise. NSPS can be computed by applying the window set to the input data to create a set of windowed wavefields, which are individually phase-shift extrapolated with the corresponding constant velocity, and the extrapolated set is superimposed. PSPI proceeds by phase-shift extrapolating the input data for each distinct velocity, applying the j th window to the j th extrapolation, and superimposing. Though neither process is fully correct, PSPI has the unphysical limit that discontinuities in the lateral velocity variation cause discontinuities in the wavefield, whereas NSPS shows the expected wavefront "healing."

We then formulate a finite aperture compensation for NSPS which has the practical result of absorbing lateral boundaries for all incidence angles. Wavefield extrapolation can be regarded as the crosscorrelation of the wavefield with the expected response of a point diffractor at the new depth level. Aperture compensation simply applies a laterally varying window to the infinite, theoretical diffraction response. The crosscorrelation becomes spatially variant, even for constant velocity, and hence is a nonstationary filter. The nonstationary effects of aperture compensation can be simultaneously applied with the NSPS extrapolation through a laterally variable velocity field.

INTRODUCTION

In a general context, wavefield extrapolation refers to the mathematical technique of advancing a wavefield through space or time. Such techniques can be used in both seismic migration and seismic modeling. In this paper, we will restrict the scope of wavefield extrapolation to the problem of deducing a scalar wavefield at one depth level in the earth given knowledge of its properties at another level. We also assume that the wave propagation velocity, v , depends only on the lateral spatial coordinates, (x, y) , and not on the depth, z . Consequently, our technique is intended for use in a recursive scheme in which

vertical velocity variations are handled in the usual manner through an appropriate choice of depth levels, and only lateral velocity variations are directly addressed by our theory.

Wavefield extrapolation by phase shift (Gazdag, 1978) has many desirable properties and one overriding difficulty. On the positive side, the phase-shift operator is theoretically exact for constant velocity, unconditionally stable, shows no grid dispersion, and is accurate for all scattering angles. (We prefer the term "scattering angle" to the more commonly used "dip" because the latter is often confused with the geologic dip of reflectors.) The major difficulty is that it is not immediately apparent how lateral velocity variations can be incorporated into

Manuscript received by the Editor October 16, 1997; revised manuscript received December 18, 1998.

*University of Calgary, Consortium for Research in Elastic Wave Exploration Seismology (CREWES) Project, 2500 University Drive N.W., Calgary, Alberta T2N 1N4, Canada. E-mail: gary@geo.ucalgary.ca; rferguso@geo.ucalgary.ca.

© 1999 Society of Exploration Geophysicists. All rights reserved.

a phase-shift method because the space coordinate has been Fourier transformed. As a result, extrapolation techniques for $v(x)$ [we use “ $v(x)$ ” as synonymous with the phrase “a laterally variable velocity field”] are usually formulated in the space-frequency domain (e.g., Gazdag, 1980; Berkhout, 1984; Holberg, 1988; Hale, 1991) as a (scattering) angle-limited approximation to the inverse Fourier transform of the phase-shift operator. The velocity dependence of such a local space-domain extrapolator is then varied with the local velocity of the computation grid. However, since the multidimensional Fourier transform is a complete description of a wavefield, it follows that it must be possible to extrapolate a wavefield through lateral velocity variations with a Fourier domain technique. We present such a technique here and illustrate its relation to established methods. Black et al. (1984) and Wapenaar (1992) have presented similar Fourier methods (see also Wapenaar and Dessing, 1995, and Grimbergen et al., 1995).

The split-step Fourier method (Stoffa et al., 1990) and the similar phase-screen methods (Wu, 1994; Huang and Wu, 1996; Huang and Fehler, 1997) are related but distinct from the methods described here. These phase-screen methods split the extrapolation into two parts: an angle-independent thin-lens delay (accomplished in the space-frequency domain) and an angle-dependent scattering (accomplished in the full-Fourier domain). The thin-lens delay is computed with the actual lateral velocity variations, whereas the Fourier domain scattering is done using a constant background velocity. The method presented here does not separate scattering from thin-lens delay nor does it require a constant velocity background. Instead, wavefield extrapolation by nonstationary phase shift (NSPS) can be done entirely in the Fourier domain with the actual lateral velocity variation.

We present our work in the context of nonstationary filter theory (Margrave, 1998), and show its analytic link to the popular phase shift plus interpolation (PSPI) method of Gazdag and Squazzero (1984). NSPS is presented as an explicit closed-form expression for one-way wavefield extrapolation through $v(x)$ and has the physical interpretation of a laterally varying, or nonstationary, phase shift. Next, we give a detailed comparison between NSPS and PSPI for the case of a step velocity model. As a further demonstration of the utility of our approach, we conclude with a modification of NSPS which has perfectly absorbing (that is, reflections are suppressed at all dips) lateral boundaries. This is achieved through the compensation of the NSPS operator for finite recording aperture. Finally, we discuss practical extensions of this technique to 3-D wavefield extrapolation.

THEORETICAL DEVELOPMENT

We begin with a summary of PSPI and show how to formulate the most accurate, limiting form of PSPI as a generalized Fourier integral. Then, using results from the theory of nonstationary linear filters, we show that the PSPI limiting form is a type of nonstationary filter called a combination filter. Such filters are linear and have definable properties; however, they do not form the linear superposition of impulse responses which Huygen’s principle suggests is desirable in wave propagation. This motivates the use of a nonstationary convolution filter that does form the desired linear superposition and is the basis for our NSPS algorithm. We give expressions for NSPS and PSPI

in the dual (space-wavenumber) domain and in the full-Fourier domain.

The PSPI method

PSPI (Gazdag and Squazzero, 1984) is a rational attempt to build an approximate extrapolation through $v(x)$ from a set of constant velocity phase-shift extrapolations using a suitable set of reference velocities, $\{v_j\}$. For simplicity, we present the theory in two dimensions as the extrapolation of a wavefield from $z = 0$ to $z = \Delta z$. (A summary of our mathematical notation appears in Appendix A.) After an initial Fourier transform over time, we denote the wavefield at $z = 0$ as $\Psi(x, 0, \omega)$, where ω is temporal frequency, and the desired extrapolated wavefield at $z = \Delta z$ as $\Psi_{v(x)}(x, \Delta z, \omega)$, where the subscript provides information about the velocity field. Phase-shift extrapolation with each v_j produces a reference wavefield, $\Psi_{v_j}(x, \Delta z, \omega)$, given by

$$\Psi_{v_j}(x, \Delta z, \omega) = \int_{-\infty}^{\infty} \varphi(k_x, 0, \omega) \alpha_{v_j}(k_x, \omega) e^{ik_x x} dk_x, \quad (1)$$

where

$$\varphi(k_x, 0, \omega) = \frac{1}{2\pi} \int_{-\infty}^{\infty} \Psi(x, 0, \omega) e^{-ik_x x} dx \quad (2)$$

is the forward spatial Fourier transform of the input data, the phase-shift operator, α_{v_j} , is given by

$$\alpha_{v_j}(k_x, \omega) = \begin{cases} e^{i\Delta z k_{zj}}, & |k_x| \leq \frac{\omega}{v_j} \\ e^{-|\Delta z k_{zj}|}, & |k_x| > \frac{\omega}{v_j} \end{cases}, \quad k_{zj} = \sqrt{\frac{\omega^2}{v_j^2} - k_x^2}, \quad (3)$$

and k_x and k_z are horizontal and vertical wavenumbers, respectively. This definition of α_{v_j} ensures that evanescent energy suffers exponential decay. Note that each reference wavefield, Ψ_{v_j} is a complete phase-shift extrapolation defined at all x and ω although we do not expect it to contribute to $\Psi_{v(x)}$ where $v(x)$ differs significantly from v_j . It is a fundamental assumption of PSPI that the desired extrapolation is equivalent to a reference wavefield wherever the actual velocity equals the reference velocity. That is,

$$\Psi_{v(x)}(x_j, \Delta z, \omega) = \Psi_{v_j}(x_j, \Delta z, \omega), \quad \text{if } v(x_j) = v_j. \quad (4)$$

PSPI proceeds by choosing a small set of reference velocities that bracket the extremes of $v(x)$ and sample its fluctuations. Once the set $\{\Psi_{v_j}\}$ is determined, an approximation to $\Psi_{v(x)}$ is formed by some sort of linear (in velocity) interpolation (LI),

$$\Psi_{v(x)}(x, \Delta z, \omega) \approx \text{LI}(\Psi_{v_j}(x, \Delta z, \omega), \Psi_{v_{j+1}}(x, \Delta z, \omega)), \quad v_j \leq v(x) \leq v_{j+1}. \quad (5)$$

The choice of the reference velocities and the details of the interpolation process symbolized by equation (5) are major technical design questions because they control the accuracy of the final result. However, we are not concerned with them here because we wish to proceed to the most accurate limiting case of PSPI, when a reference wavefield is computed for every

distinct velocity. In this case, the PSPI algorithm converges to

$$\begin{aligned} \Psi_{v(x)}(x, \Delta z, \omega) &\approx \Psi_{\text{PSPI}}(x, \Delta z, \omega) \\ &= \int_{-\infty}^{\infty} \varphi(k_x, 0, \omega) \alpha_{v(x)}(k_x, x, \omega) e^{ik_x x} dk_x, \end{aligned} \quad (6)$$

where

$$\alpha_{v(x)}(k_x, x, \omega) = \begin{cases} e^{i\Delta z k_z(x)}, & |k_x| \leq \frac{\omega}{v(x)} \\ e^{-|\Delta z k_z(x)|}, & |k_x| > \frac{\omega}{v(x)} \end{cases}, \quad k_z(x) = \sqrt{\frac{\omega^2}{v(x)^2} - k_x^2}. \quad (7)$$

Note that we reserve the symbol Ψ_{PSPI} to refer specifically to the most accurate limiting form of PSPI as expressed by equation (6). For the remainder of this paper, when we use the term PSPI, we will be referring to a computation done with equation (6) (or a mathematical equivalent). Equation (6) is essentially similar to equation (1) except that the constant velocity, v , in the latter has become $v(x)$ in the former. This means that equation (6) is no longer an inverse Fourier transform but is a more general Fourier integral. It can be interpreted as a prescription which applies the nonstationary filter of equation (7) simultaneously with the transformation from k_x to x . In order to appreciate the validity of this result, it is useful to explicitly verify that equation (4) is satisfied:

$$\Psi_{\text{PSPI}}(x_j, \Delta z, \omega) = \Psi_{v_j}(x_j, \Delta z, \omega), \quad x_j \Rightarrow v(x_j) = v_j. \quad (8)$$

Thus the limiting PSPI wavefield, as given by equation (6), is equivalent to producing a complete set of reference velocities and extrapolated wavefields, then slicing through the wavefields such that each is used only where its velocity equals $v(x)$. This is illustrated in Figure 1. An alternative to this slicing process, is the direct numerical integration of equation (6). In this limiting case, the problems of reference velocity selection and choice of interpolation algorithm vanish.

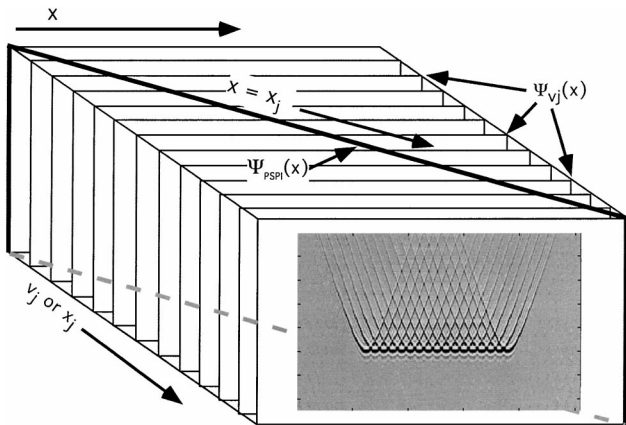


FIG. 1. The limiting form of PSPI produces a continuous set of extrapolated wavefields $\Psi_{v_j}(x)$, one for each v_j . The final extrapolated wavefield $\Psi_{\text{PSPI}}(x)$ is the set of traces found along a slice at $x = x_j$ through the data volume.

The NSPS method

The theory of nonstationary linear filters, as presented in Margrave (1998), shows that at least two distinct forms of nonstationary filters are possible. Termed combination and convolution filters, both filter forms are equivalent in the stationary limit—in this context, stationary means constant velocity—but otherwise they can differ dramatically. The theory gives explicit prescriptions for filter application in the space, Fourier, or dual domains as well as formulas to move the filter prescription between domains. (A dual-domain filter expression is one which changes the data domain from space to Fourier, or the reverse, in the process of applying the filter.)

As described above, Ψ_{PSPI} is computed by an ordinary forward Fourier transform, equation (2), and then the generalized inverse Fourier integral, equation (6), and is an example of a nonstationary, dual-domain, combination filter. The nonstationarity of the filter is evidenced by the fact that the filter description, $\alpha_{v(x)}(k_x, x, \omega)$, is dependent upon both wavenumber and spatial location. (The spatial dependence vanishes for a stationary filter.)

The distinction between combination and convolution filter forms is most apparent in the dual-domain form. Given equation (6) and following the nonstationary filter theory, it is now a simple matter to write the equations describing the related nonstationary convolution filter. The first step applies the nonstationary wavefield extrapolator, $\alpha_{v(x)}$, given by equation (7), simultaneously with the forward Fourier transform

$$\begin{aligned} \varphi_{\text{NSPS}}(k_x, \Delta z, \omega) &= \frac{1}{2\pi} \int_{-\infty}^{\infty} \Psi(x, 0, \omega) \alpha_{v(x)}(k_x, x, \omega) e^{-ik_x x} dx. \end{aligned} \quad (9)$$

The final step is an ordinary inverse Fourier transform:

$$\Psi_{\text{NSPS}}(x, \Delta z, \omega) = \int_{-\infty}^{\infty} \varphi_{\text{NSPS}}(k_x, \Delta z, \omega) e^{ik_x x} dk_x. \quad (10)$$

Equations (9) and (10) form the basis of our method of wavefield extrapolation by nonstationary phase shift. In comparison with the limiting form of PSPI, both methods apply the same nonstationary filter, $\alpha_{v(x)}$ as given by equation (7), but NSPS applies it simultaneously with the forward Fourier transform from x to k_x , whereas in PSPI it is applied simultaneously with the inverse Fourier transform from k_x to x . In the stationary limit, when $\alpha_{v(x)}$ becomes independent of x , it is a simple matter to verify that both expressions reduce to the constant velocity phase-shift extrapolation.

Although we have based our presentation on the concepts of nonstationary filter theory, we note that these are closely linked to the theory of pseudodifferential operators (Saint Raymond, 1991) and the related Fourier integral operators (Duistermaat, 1996). In fact, equation (6) is a Fourier integral operator in standard form, and equation (9) can be shown to be the adjoint form.

Fourier domain formulation

At this point, both the PSPI limiting process and NSPS have been presented as dual-domain algorithms which have the characteristic that the nonstationary extrapolation filter

is applied simultaneously with a data transformation from wavenumber to space or the reverse. Nonstationary filter theory provides the mathematical formulas to move either process fully into the Fourier domain [where the input and output wavefields are in (k_x, ω)] or into the space domain [where the wavefields are in (x, ω)]; however, we present only the Fourier domain expressions here.

The space-domain (x, ω) expressions for NSPS and PSPI can be derived through mathematics similar to that presented here. For discrete data, it can be shown that NSPS and PSPI are accomplished with extrapolation matrices that are the transpose of one another. Curiously, this transpose symmetry does not hold in the full-Fourier domain. This is because $\alpha_{v(x)}(k_x, x, \omega)$, as given by equation (7), is symmetric in k_x [i.e., $\alpha(k_x) = \alpha(-k_x)$] but not in x .

PSPI can be moved into the Fourier domain by performing the forward Fourier transform of equation (6) (Appendix B). This results in

$$\varphi_{\text{PSPI}}(k_x, \Delta z, \omega) = \int_{-\infty}^{\infty} \varphi(k'_x, 0, \omega) A(k'_x, k_x - k'_x, \omega) dk'_x, \quad (11)$$

where

$$A(p, q, \omega) = \frac{1}{2\pi} \int_{-\infty}^{\infty} \alpha_{v(x)}(p, u, \omega) e^{-iq u} du. \quad (12)$$

In equation (12), p and q are wavenumber variables and u is a space coordinate. The wavenumber connection function, A , is seen to be the ordinary forward Fourier transform over the spatial coordinate of $\alpha_{v(x)}$.

The Fourier expression for NSPS (Appendix C) is derived from equation (9) by substituting for Ψ its expression as an inverse Fourier transform of its spectrum, φ . The result is

$$\varphi_{\text{NSPS}}(k_x, \Delta z, \omega) = \int_{-\infty}^{\infty} \varphi(k'_x, 0, \omega) A(k_x, k_x - k'_x, \omega) dk'_x, \quad (13)$$

where A is given by equation (12).

Equations (11) and (13) are very similar, differing only in how the p dependence of $A(p, q)$ is mapped into (k_x, k'_x) space. For discretely sampled data, both of these extrapolation equations can be represented as matrix operations in which an extrapolation matrix populated from $A(p, q)$ is multiplied into a column vector containing samples of φ . In the stationary limit [i.e., $v(x) = \text{constant}$], both of the extrapolation matrices become diagonal with the phase-shift extrapolator appearing on the diagonal. As $v(x)$ is allowed to vary, off-diagonal terms appear in the matrices and, when multiplied into the data vector, cause a "mixing" of the wavenumbers of φ to produce each wavenumber of $\varphi_{v(x)}$. An alternative perspective is that $\alpha_{v(x)}$ represents a phase-shift model based on the velocity model $v(x)$. These formulas [equations (11) and (13)] prescribe how the wavenumbers of the phase-shift model, and hence indirectly the velocity model, mix with the wavenumbers of the data during wavefield extrapolation.

The strong similarity of equations (11) and (13) suggests that the computational effort for PSPI and NSPS is nearly identical [recall that we speak of the generalized PSPI here as defined by equation (6)]. Both methods require a forward Fourier trans-

form of the input wavefield and an inverse Fourier transform of the extrapolated field. The wavenumber connection function, A , is constructed identically for both as the forward Fourier transform of α [equation (12)]. The only difference is in the application of A . In a digital application using matrices, the efficiency of the calculation of equation (12) is increased if α is stored with u as the row coordinate so that each Fourier transform operates on a vector in contiguous memory. The resulting matrix is optimal for computation of equation (11) by matrix-vector multiplication but must be transposed to compute equation (12). The conclusion that there may be a slight efficiency advantage for PSPI depends on the assumption that the Fourier transform of contiguous data is significantly more efficient than for separated data elements. This may not always be the case, especially for highly vectorized hardware. Our experience (with Matlab on Sun workstations) shows the two methods have identical floating point operations counts and only slightly different CPU times.

We emphasize that these Fourier-domain expressions will give theoretically identical results to the dual-domain formulas or to space-domain results. However, the formulas are distinct from a numerical perspective because each domain has its potential strengths and weaknesses in a particular computational setting. A potential advantage of this Fourier approach is the possibility of gaining efficiency for smooth velocity models by computing and applying only a limited number of off-diagonal terms.

COMPARISON OF NSPS AND PSPI

The formal demonstration that nonstationary convolution forms the linear superposition of the nonstationary filter impulse response, whereas nonstationary combination does not, is given in Margrave (1998). Here, we will take a more conceptual approach. Consider the computation of both Ψ_{NSPS} and Ψ_{PSPI} in the case when the nonstationary phase-shift operator is given by

$$\alpha_{v(x)}(k_x, x, \omega) = \begin{cases} \alpha_{v_1}(k_x, \omega), & x < 0 \\ \alpha_{v_2}(k_x, \omega), & x \geq 0 \end{cases}, \quad (14)$$

where α_{v_1} and α_{v_2} are two different constant velocity phase-shift operators corresponding to velocities v_1 and v_2 as given by equation (3). We will give an analytic analysis and show numerical examples. (All of our numerical examples were computed using the full-Fourier method just discussed.)

Figure 2 shows the numerical test case that we will use to illustrate the conceptual results. The seismic section shown contains a horizontal line of impulses with a zero pad attached to both sides to avoid operator wraparound, as is customary for Fourier methods. The velocity model is 5000 m/s on the left, and changes discontinuously in the middle of the section to 2000 m/s. The wavefield extrapolations to be shown will all use a 50-m downward extrapolation step. For comparison with NSPS and PSPI, Figure 3a shows an ordinary phase-shift extrapolation using the intermediate velocity of 3500 m/s. Figure 3b shows the amplitude spectrum of the Fourier extrapolation matrix for a particular frequency, ω . As discussed previously, it is a purely diagonal matrix whose nonzero elements contain the phase-shift

extrapolator, α_{vj} [equation (3)]. Multiplication of the input wavefield, represented as a column vector of wavenumber components for a single frequency, results in a column vector of the output wavefield with no wavenumber mixing.

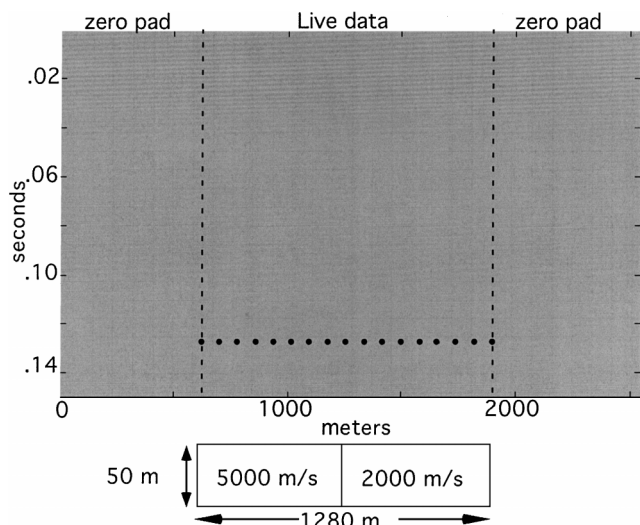


FIG. 2. Numerical test case showing impulses to be extrapolated through a discontinuous velocity model. “Live data” refers to the input wavefield; “zero pad” refers to the zero pad in x required by the Fourier domain extrapolation.

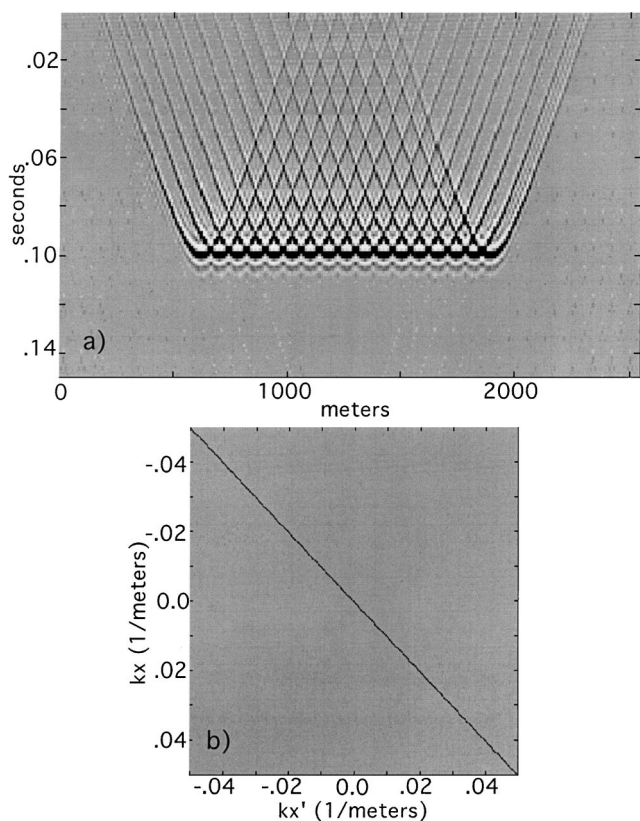


FIG. 3. (a) Phase-shift extrapolation for the numerical test case of Figure 2 using constant velocity ($v = 3500$ m/s). (b) Amplitude spectrum of Fourier extrapolation matrix for a particular ω in the constant velocity case.

Next, we compute Ψ_{PSPI} by substituting equation (14) into equation (6). After some elementary manipulations, we obtain

$$\Psi_{\text{PSPI}}(x, \Delta z, \omega) = \begin{cases} \Psi_{v1}(x, \Delta z, \omega), & x < 0 \\ \Psi_{v2}(x, \Delta z, \omega), & x \geq 0 \end{cases}, \quad (15)$$

where Ψ_{v1} and Ψ_{v2} are reference wavefields for α_{v1} and α_{v2} computed from equation (1). Equation (15) shows that Ψ_{PSPI} is the discontinuous juxtaposition of two reference wavefields. Margrave (1998) shows that nonstationary combination filters generally have the property that lateral discontinuities in filter specifications will cause similar discontinuities in the filtered result. This is a nonphysical behavior since a superposition of Huygen’s wavelets should always smooth over discontinuities.

Figure 4a shows Ψ_{PSPI} for our numerical test case. The central discontinuity is clearly obvious, as is the dramatic difference in traveltime delay between the left and right sides. If this result were input into a subsequent extrapolation step, the discontinuity would cause objectionable wavefronting. Note also that the hyperbolic impulse responses show two different curvatures. Figure 4b is the amplitude spectrum of the Fourier extrapolation matrix for the same frequency as in Figure 3b. The nonzero off-diagonal terms are clearly evident, although it is interesting to note that, even for this discontinuous velocity model, they quickly decrease away from the diagonal.

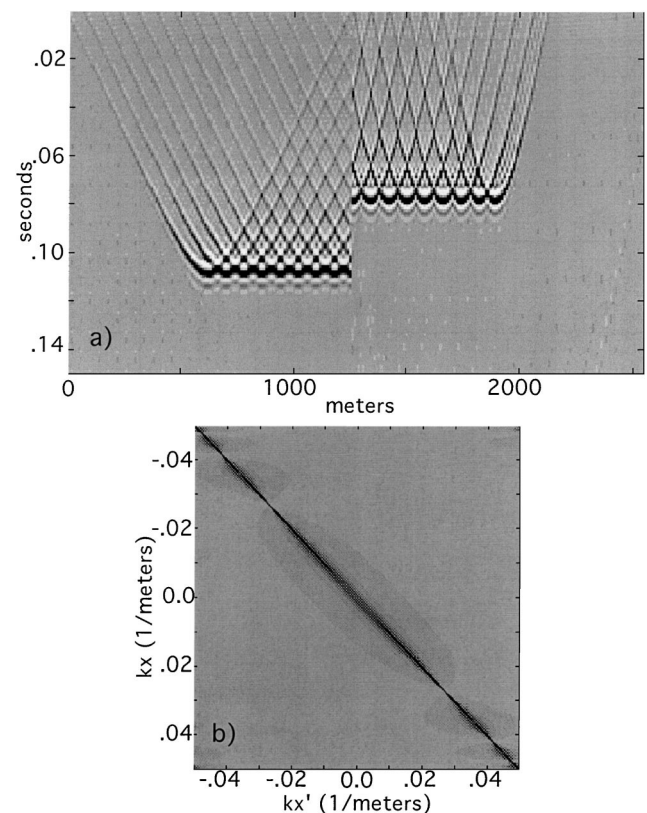


FIG. 4. (a) Ψ_{PSPI} for the numerical test case of Figure 2. The discontinuity in the output wavefield in the figure corresponds to the discontinuity in the velocity field. (b) Amplitude spectrum of the PSPI extrapolation matrix for a particular ω . Laterally varying velocities generate off-diagonal terms.

Next, consider Ψ_{NSPS} by substituting equation (14) into equation (9) and breaking the integral into two parts to get

$$\begin{aligned} \varphi_{\text{NSPS}}(k_x, \Delta z, \omega) = & \frac{1}{2\pi} \left[\alpha_{v1}(k_x, \omega) \right. \\ & \times \int_{-\infty}^{0^-} \Psi(x, 0, \omega) e^{ik_x x} dx + \alpha_{v2}(k_x, \omega) \\ & \left. \times \int_0^{\infty} \Psi(x, 0, \omega) e^{-ik_x x} dx \right]. \end{aligned} \quad (16)$$

Now define two differently windowed versions of the input wavefield:

$$\Psi|_{v1}(x, 0, \omega) = \begin{cases} \Psi(x, 0, \omega), & x < 0 \\ 0, & x \geq 0 \end{cases}$$

and (17)

$$\Psi|_{v2}(x, 0, \omega) = \begin{cases} 0, & x < 0 \\ \Psi(x, 0, \omega), & x \geq 0 \end{cases}$$

Then, equation (16) can be written

$$\begin{aligned} \varphi_{\text{NSPS}}(k_x, \Delta z, \omega) = & \alpha_{v1}(k_x, \omega) \varphi|_{v1}(k_x, 0, \omega) \\ & + \alpha_{v2}(k_x, \omega) \varphi|_{v2}(k_x, 0, \omega), \end{aligned} \quad (18)$$

where $\varphi|_{v1}$ and $\varphi|_{v2}$ are the ordinary Fourier transforms of $\Psi|_{v1}$ and $\Psi|_{v2}$, respectively. Ψ_{NSPS} is simply the inverse Fourier transform of φ_{NSPS} as in equation (10). Since the inverse Fourier transform is linear, it can be distributed over the sum in equation (18). This analysis shows that Ψ_{NSPS} may be computed by “windowing” the input wavefield as in equation (17) to isolate those portions spatially coincident with each distinct velocity, extrapolating the windowed wavefields with phase shifts, and superimposing the results.

Figure 5a shows Ψ_{NSPS} for the numerical test case. Unlike Figure 4a, there is no central discontinuity, and each input impulse has been replaced by the time-reversed diffraction response characteristic of the local velocity. This is a more physically plausible result than that of Figure 4a and can be seen to be in qualitative agreement with Huygen’s principle. However, it is still not fully correct as the diffraction responses do not show refractions at the velocity boundary. In comparison with Figure 4a, it is apparent that PSPI does refract the diffraction limbs but at the cost of introducing discontinuities in the wavefield. Figure 5b is the Fourier matrix that achieves NSPS extrapolation. As mentioned previously, the NSPS and PSPI matrices are not quite transposes of one another in the full-Fourier domain. The NSPS matrix can be formed by transposing the PSPI matrix and then flipping each row about the diagonal [compare equations (11) and (13)].

To accentuate the comparison, Ψ_{PSPI} [equation 15] can be rewritten to incorporate an explicit windowing step as well by

defining

$$\Psi_{v1|v1}(x, \Delta z, \omega) = \begin{cases} \Psi_{v1}(x, \Delta z, \omega), & x < 0 \\ 0, & x \geq 0 \end{cases}$$

and (19)

$$\Psi_{v2|v2}(x, \Delta z, \omega) = \begin{cases} 0, & x < 0 \\ \Psi_{v2}(x, \Delta z, \omega), & x \geq 0 \end{cases},$$

then

$$\Psi_{\text{PSPI}}(x, \Delta z, \omega) = \Psi_{v1|v1}(x, \Delta z, \omega) + \Psi_{v2|v2}(x, \Delta z, \omega). \quad (20)$$

So, PSPI and NSPS can be contrasted by where, in the process, the windowing step occurs. In NSPS, the input dataset is windowed to create the set $\{\Psi|_{vj}\}$, each member of the set is phase-shift extrapolated with the corresponding member of $\{v_j\}$, and the results are superimposed. In PSPI, the set $\{\Psi_{vj}\}$ is created by phase-shift extrapolating Ψ with each member of $\{v_j\}$, each member of $\{\Psi_{vj}\}$ is then windowed giving the set $\{\Psi_{vj|vj}\}$, and the results superimposed. The windowing functions are the same in both algorithms. This computation

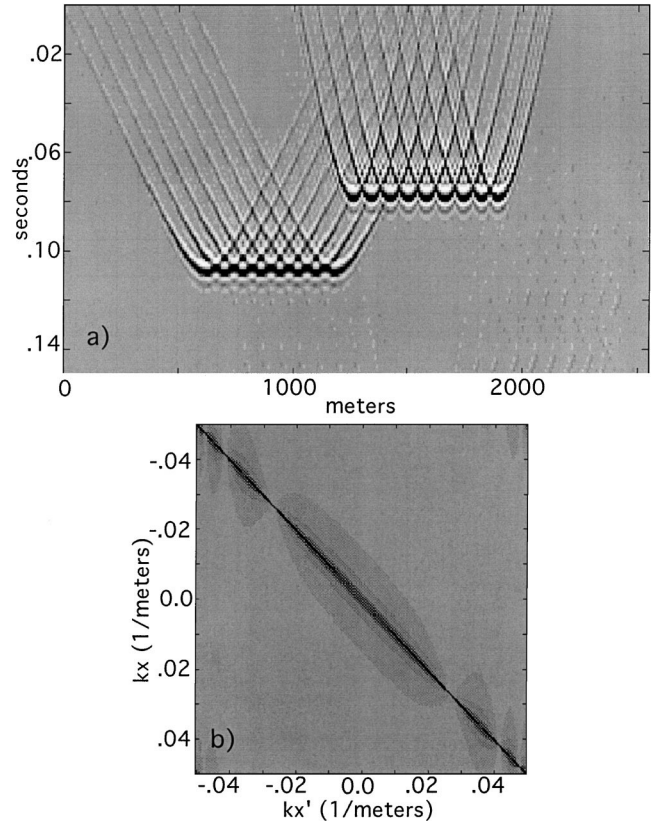


FIG. 5. (a) Ψ_{NSPS} for the numerical test case of Figure 2. The discontinuity in the velocity field is not imposed on the output wavefield. Instead, the response is a smooth superposition of wavefields. (b) Amplitude spectrum of the NSPS extrapolation matrix for a particular ω . Laterally varying velocities generate off-diagonal terms. Note the similarity of the spectrum to that of the PSPI extrapolator; in fact, they differ only by a matrix transpose and reversal of each resulting row about the center diagonal.

procedure is exact for both Ψ_{PSPI} and Ψ_{NSPS} whenever the velocity variation is piecewise constant, and illustrates again that the computational effort required for NSPS is very similar to that required for PSPI.

This analysis can be generalized to nearly arbitrarily complicated velocity variations (as long as the number of distinct velocities is countable) by defining the windowing function:

$$\Omega_j(x) = \begin{cases} 1, & v(x) = v_j \\ 0, & \text{otherwise} \end{cases} \quad (21)$$

Then, Ψ_{NSPS} can be written

$$\begin{aligned} &\Psi_{\text{NSPS}}(x, \Delta z, \omega) \\ &= \text{IFT}_{k_x \Rightarrow x} \left[\sum_j \alpha_{vj}(k_x, \omega) \text{FT}_{x \Rightarrow k_x} (\Omega_j(x) \Psi(x, 0, \omega)) \right], \end{aligned} \quad (22)$$

while Ψ_{PSPI} is

$$\begin{aligned} &\Psi_{\text{PSPI}}(x, \Delta z, \omega) = \\ &\sum_j \Omega_j(x) \text{IFT}_{k_x \Rightarrow x} [\alpha_{vj}(k_x, \omega) \text{FT}_{x \Rightarrow k_x} (\Psi(x, 0, \omega))]. \end{aligned} \quad (23)$$

In these expressions, FT and IFT are forward and inverse Fourier transforms, and the sum is over the complete set of distinct velocities. Equations (22) and (23) define the windowing analog for the computation of NSPS and PSPI, respectively. In the constant velocity case, the equivalence of both methods with ordinary phase shift can be easily appreciated since Ω_j becomes unity and the sums collapse to a single term.

Figure 6 shows Ψ_{NSPS} and Ψ_{PSPI} for the complicated velocity function shown in Figure 6c. The NSPS result is clearly more coherent than that from PSPI. [In fairness, we note that a practical implementation PSPI would never be run with such rapid lateral velocity variations. Instead, a few reference wavefields would be computed, and a smoothed interpolated result would be obtained from equation (5). Thus the result would be less chaotic than that shown in Figure 6b but also less accurate than that shown in Figure 6a.]

The reason for the relatively chaotic nature of the PSPI extrapolations compared with NSPS can be appreciated from the windowing analog. In the former case, phase-shift wavefield extrapolation (with evanescent filtering) precedes windowing and the windowing creates evanescent energy. In the NSPS case, the final step is phase-shift extrapolation so the result is properly filtered for evanescent energy. In a multistep scheme, the PSPI result of Figure 6b would be immediately subjected to an evanescent filter in a second step that will reduce its chaotic appearance. After multiple steps through complex velocity models, the differences between NSPS and PSPI become more subtle.

APERTURE COMPENSATION

Intuitively, the reason that nonstationary theory is required for vertical wavefield extrapolation through $v(x)$ is that the wavefield extrapolation operator changes spatially as $v(x)$ varies. It follows that any other space and wavenumber variant processes may be incorporated into the extrapolation operator in similar fashion. One such process is the implementation of absorbing lateral boundaries. Absorbing boundaries

have been developed quite successfully for finite difference and other space-domain methods (Clayton and Engquist, 1977; Keys, 1985), and we extend them to Fourier methods here. The usual concept is to alter the dispersion relation of waves near the boundary such that only outward traveling wavefronts are allowed; however, this is usually not possible for all propagation angles (Claerbout, 1985). We achieve absorbing boundaries for all propagation angles from the viewpoint of developing an extrapolation operator that is compensated for finite recording aperture.

Aperture compensation follows from an understanding of the downward extrapolation of upward traveling waves as a

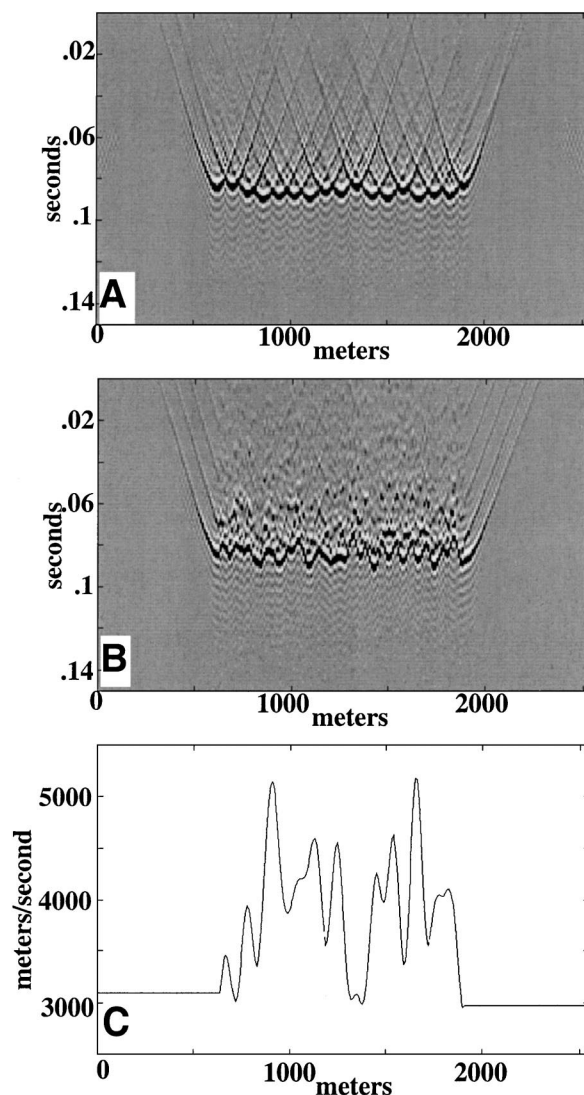


FIG. 6. (a) Ψ_{NSPS} for complicated velocity variation. The wavefield of Figure 2 was used as input to NSPS extrapolation through the complicated (though arbitrary) velocity of (c). The resulting NSPS wavefield is a continuous superposition of diffraction responses. (b) Ψ_{PSPI} for complicated velocity variation. The wavefield of Figure 2 was used as input to PSPI extrapolation through the complicated velocity of (c). The chaotic response of the extrapolation is conceptually the result of windowing a set of constant velocity extrapolations and combining them into an output section. (c) Complicated velocity function used to compare NSPS and PSPI.

process of crosscorrelation with an appropriate diffraction response. The inverse Fourier transform of the phase-shift operator is essentially the diffraction response of the scalar wave equation (Robinson and Silvia, 1981, p. 370). From here, it is not difficult to show that the space-time equivalent of phase-shift downward continuation is a convolution with a time-reversed diffraction response (hyperbola), as shown in Figure 7a. Equivalently, this can be regarded as a crosscorrelation with the time-normal diffraction response. Thus a very appealing picture emerges: the downward continuation of upward traveling waves from depth z_1 to depth z_2 can be done by crosscorrelation of the wavefield recorded at z_1 with the expected response of a point scatterer at z_2 .

We can regard any seismic line as a spatial window that allows only a portion of the response of a point scatterer at z_2 to be recorded at z_1 . We deduce that a better crosscorrelation operator than the normal infinite, symmetric operator would be that operator with an appropriate spatial window applied. It follows immediately that aperture-compensated downward continuation must be a nonstationary process even in the constant velocity case because the expected windowed diffraction response must vary laterally.

Consider a seismic line, recorded at z_1 , where the only reflecting element is a point scatterer at z_2 near the left edge of the line (Figure 7b). The expected zero-offset response is the right-hand limb of a diffraction hyperbola. Downward continuation by crosscorrelation with a symmetric hyperbola (simulating, perhaps, a limited scattering angle operator) is shown in Figure 7c (the temporal delay of the operator is not shown so that the focusing effects can be more clearly appreciated). The use of an aperture-compensated operator is shown in Figure 7d, where the crosscorrelation is done with the expected windowed diffraction response. The crosscorrelation is shown as a convolution-by-replacement with the time-and-space-reversed diffraction response.

An extrapolation operator that has been aperture compensated varies from completely left-sided on the left end of a seismic line, to symmetric in the middle, and then to completely right-sided on the right end. This means that the operator has a scalar wave-dispersion relation that varies smoothly from a left or right quarter circle on either end to symmetric in the middle. This is exactly the "Engquist boundary condition" for absorbing lateral boundaries discussed by Claerbout (1985). Thus absorbing boundaries arise as a natural consequence of aperture compensation and, additionally, a smooth lateral variation of the dispersion relation is obtained.

A one-sided diffraction response has a one-sided $\omega-k_x$ spectrum. Viewing crosscorrelation as a multiplication of $\omega-k_x$ spectra, it is easy to appreciate that the crosscorrelation of a one-sided diffraction with a two-sided diffraction will produce the same result as the crosscorrelation of the one-sided diffraction with itself. The problem with the symmetric operator stems from the fact that seismic data generally contains energy at all k_x values, even near the aperture boundaries, due primarily to noise. Thus, the symmetric operator can produce "false correlations" near the boundaries which appear as wavefronts "reflecting" from the boundary. Such events are unphysical as they represent reflector dips that could not possibly have been recorded by the finite-aperture seismic line. The one-sided operator cannot produce such events.

We formulate an aperture-compensated extrapolation operator by directly limiting its spectral content as a function of position. As shown in Figure 8, the finite aperture can be regarded as a space-variant scattering-angle filter where the

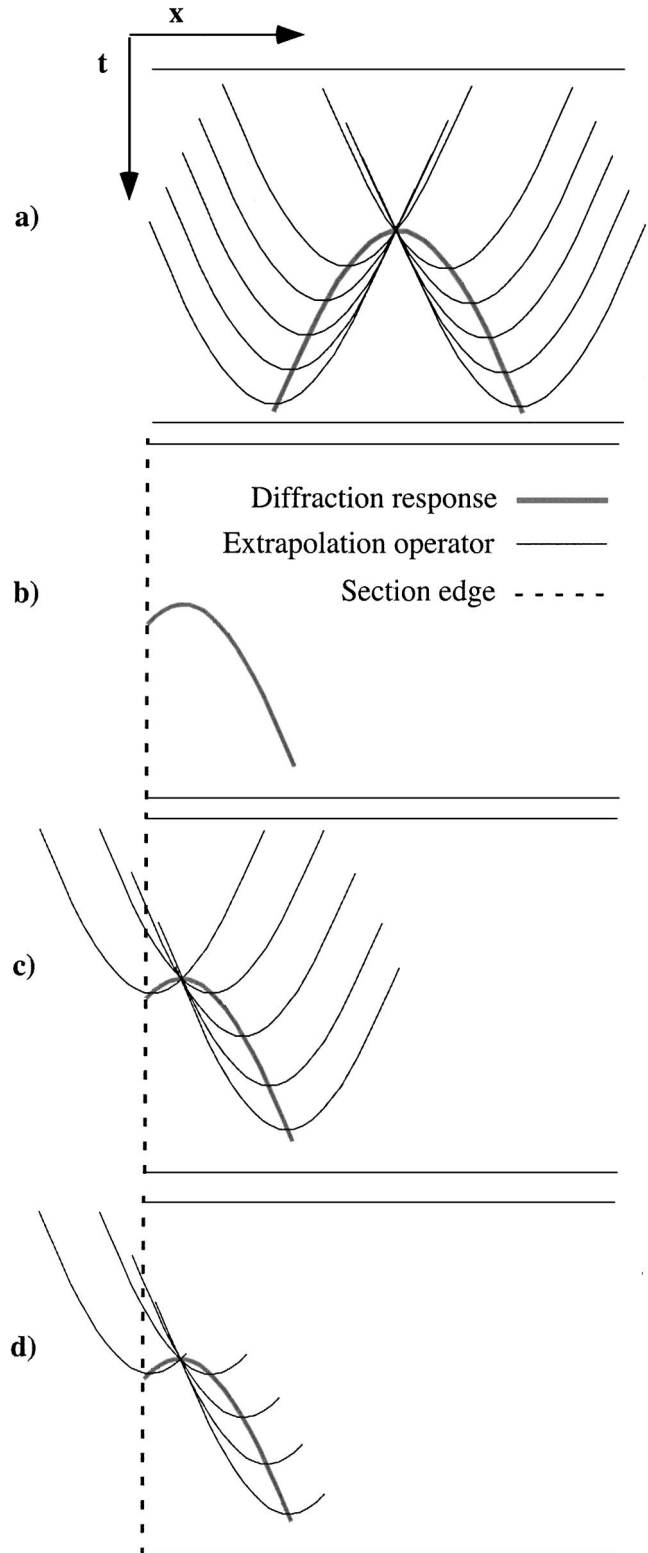


FIG. 7. (a) Application of the downward continuation operator considered as a convolution of the recorded wavefield at one depth with the time and space reversed response of a point scatterer at another depth. (The extrapolation time shift has been ignored to simplify comparison.) (b) Diffraction response near the edge of the recording aperture. (c) Downward continuation of a diffraction response at the edge of the recording aperture using a symmetric operator. Residual wavefronts will be generated by this process and will appear as boundary reflections. (d) Downward continuation using an aperture-compensated operator, resulting in a perfectly absorbing boundary.

left and right scattering-angle limits correspond to raypaths from a scatterpoint to either end of the line. Approximating these raypaths as straight rays, this filter can be expressed as

$$\beta(k_x, x, \omega) = \begin{cases} 1, & -\omega \sin(\theta_L) \leq v(x)k_x \leq \omega \sin(\theta_R) \\ 0, & \text{otherwise} \end{cases}, \quad (24)$$

where θ_L and θ_R are left and right scattering angles as defined in Figure 8. Then, the aperture-compensated operator can be written:

$$\alpha_{v(x)}^{\text{aper}}(k_x, x, \omega) = \beta(k_x, x, \omega)\alpha_{v(x)}(k_x, x, \omega). \quad (25)$$

Using $\alpha_{v(x)}^{\text{aper}}$ in place of $\alpha_{v(x)}$ in equation (9) or equation (12) implements aperture compensation in either the dual or Fourier domains.

Figure 9a shows Ψ_{NSPS} computed with aperture compensation where the aperture is defined as the live data zone of Figure 2. Careful inspection shows that the impulse responses on both edges are completely one-sided, having only an outgoing wavefront. The second impulse response in from each edge is also slightly modified. Figure 9b shows amplitude spectrum of the Fourier extrapolation matrix, and it is obvious that aperture compensation has been purchased at the expense of a considerable increase in off-diagonal power.

Finally, we note that a Fourier method actually has two mechanisms that can lead to similar wavefronting near the boundary. In addition to the effect discussed above, there is the possibility of “operator wraparound” resulting from an insufficient lateral zero pad. As formulated here, our method of aperture compensation still requires an adequate zero pad, although its suppression with a further nonstationary operator appears possible.

EXTENSION TO THREE DIMENSIONS

To this point, we have considered only the extrapolation of 2-D wavefields and have shown results computed with the full-Fourier domain equations (11) and (13). As discussed, the digital implementation of these equations can be formulated as a matrix multiplication, which means that a 2-D (k_x, k'_x) operator is required to handle the lateral variations along a single spatial axis. Therefore, it appears that a 3-D implementation of NSPS, addressing lateral variations in both x and y , will require a 4-D

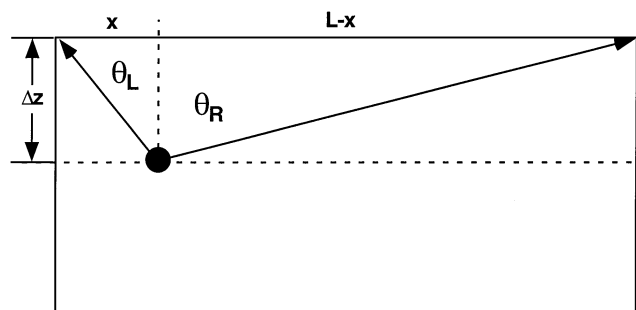


FIG. 8. An aperture-compensating (absorbing-boundary) filter is a laterally varying (nonstationary) ω - k_x fan filter defined by the maximum scattering angles allowed by the given aperture. Straight raypaths are assumed.

(k_x, k'_x, k_y, k'_y) operator. Though we have not yet produced a 3-D implementation, there are a number of possible strategies which circumvent this memory-intensive algorithm. We mention several of them here.

Perhaps the simplest approach is to directly implement the approximate windowing expression, equation (22), which is based on the assumption of a piecewise constant-velocity variation. This allows the extrapolation to be done with conventional 3-D phase-shift code and simple spatial windowing operations. Although the desired velocity variation may not be piecewise constant, it is a straightforward matter to approximate it with a piecewise constant function to any desired accuracy. A reasonable approach would be to find the piecewise constant approximation to $v(x, y)$ with the least number of segments which reduces the maximum phase error below a predetermined target. [Here, phase error refers to the phase difference between the exact phase as computed with a 3-D version of equation (7) using the exact velocity variation and the phase computed from the piecewise constant-velocity approximation.] The cost of an extrapolation step would be approximately the number of segments in the piecewise constant approximation times the cost of an ordinary 3-D phase shift. If the number of segments can be kept much smaller than the number of (x, y) locations, then this should be preferable to a direct numerical integration of a 3-D version of equation (9).

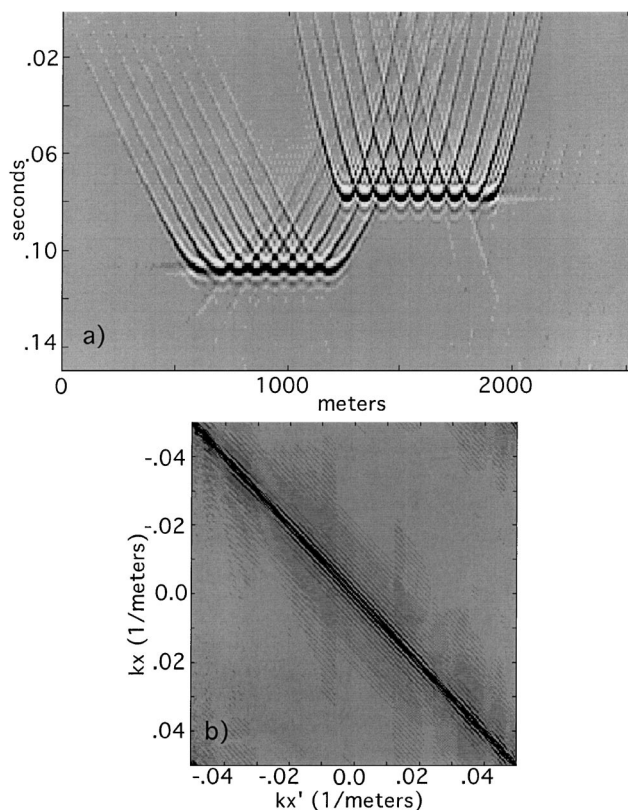


FIG. 9. (a) Ψ_{NSPS} computed including compensation for finite aperture. Impulse responses at the edges are one-sided grading to symmetric at the center of the section. (b) Amplitude spectrum of NSPS extrapolation matrix (Fourier domain). Comparison of this figure to Figure 5(b) shows the additional off-diagonal terms require for aperture compensation.

Another alternative involves developing a suitable analytic approximation to $A(p, q)$ as given by equation (12), for example perhaps by the method of stationary phase. Examination of equation (13) shows that the extrapolation operation can be considered as a weighted mix of input wavenumbers for each output wavenumber. The weights are prescribed by $A(p, q)$, which is obtained by a forward Fourier transform of $\alpha_{v(x)}(p, u)$, for which equation (7) is the analytic expression. In two dimensions, this is a 1-D mix whose weights change with output wavenumber (i.e., nonstationary). Thus, the entire A matrix need not be precomputed and held in memory; rather, it could be computed row-by-row, and each row discarded as it is used. In three dimensions, $A(p, q)$ becomes a 4-D function, say $A(p_x, q_x, p_y, q_y)$; however, its application could be viewed as a 2-D mixing operation where the 2-D array of mix weights changes with output wavenumber. Thus, the memory requirements could be reduced dramatically; however, this is computationally very demanding if A must be estimated numerically from the analytic form of α . If an approximate analytic form for A can be found, then this method becomes very attractive.

CONCLUSIONS

The vertical extrapolation of a scalar wavefield through a laterally variable velocity can be accomplished with high fidelity using a Fourier technique called nonstationary phase shift (NSPS). We assume that the wave propagation velocity, v , depends only on the lateral spatial coordinates and not on the depth. Vertical velocity variations can be addressed by using our method in a recursive progression through a series of depth levels.

The phase-shift method applies a frequency and wavenumber dependent phase shift in the Fourier domain to accomplish wavefield extrapolation through a constant velocity layer. Our NSPS method applies a similar phase shift but allows the shift to vary spatially depending upon the local propagation velocity. Both NSPS and the limiting form of phase shift plus interpolation (PSPI) can be written as generalized Fourier integrals which are examples of nonstationary linear filters and which reduce to ordinary phase shift in the constant velocity limit. However, only NSPS can be considered as a scaled, linear superposition of impulse responses (i.e., Huygen's wavelets). In the presence of strong velocity gradients, differences between the methods are dramatic though the computational effort required is similar.

When considered for the case of a piecewise constant velocity variation, NSPS can be formulated as a three-step process: (1) window the input data to isolate those portions coincident with each distinct velocity, (2) phase-shift extrapolate each windowed dataset, and (3) superimpose the results. PSPI follows a similar pattern except that the windowing is performed after each phase-shift extrapolation. Although neither extrapolation technique is fully correct, the PSPI result has discontinuities wherever the velocity is laterally discontinuous.

The nonstationary extrapolation formalism can be easily extended to include compensation for finite recording aperture. When wavefield extrapolation is viewed as the crosscorrelation of the input wavefield with the expected diffraction response at the new depth level, it becomes clear that the recording aper-

ture applies a spatially variant window to the expected diffraction response. Aperture compensation can be implemented by applying a spatially variant scattering-angle filter (ω - k_x filter) to the infinite aperture operator. This can be done simultaneously with the NSPS extrapolation through a laterally variable velocity field. The result is an operator whose dispersion relation is completely one-sided on the boundaries (equivalent to completely absorbing lateral boundaries) and which grades smoothly to a symmetric response in the center of the acquisition aperture.

A straight forward 3-D implementation of NSPS can be done using a piecewise constant approximation of the actual lateral velocity variations. This requires only conventional 3-D phase-shift and spatial-windowing operations.

ACKNOWLEDGMENTS

We thank the sponsors of CREWES for their support. We also acknowledge the influence of E. V. Herbert of Chevron Corporation (now retired) for his pioneering work on an algorithm similar to PSPI.

REFERENCES

- Berkhout, A. J., 1984, Seismic migration: Imaging of acoustic energy by wave field extrapolation: Elsevier.
- Black, J. L., Su, C. B., and Wason, C. B., 1984, Steep-dip depth migration: 54th Ann. Internat. Mtg. Soc. Expl. Geophys., Expanded Abstracts, 456-457.
- Claerbout, J. F., 1985, Imaging the earth's interior: Blackwell Scientific Publications.
- Clayton, R., and Engquist, B., 1977, Absorbing boundary conditions for acoustic and elastic wave equations: Bull. Seis. Soc. Am., **67**, 1529-1540.
- Duistermaat, J. J., 1996, Fourier integral operators: Birkhauser.
- Gazdag, J., 1978, Wave equation migration with the phase-shift method: Geophysics, **43**, 1342-1352.
- , 1980, Wave equation migration with the accurate space derivative method: Geophys. Prosp., **28**, 60-70.
- Gazdag, J., and Squazzero, P., 1984, Migration of seismic data by phase shift plus interpolation: Geophysics, **49**, 124-131.
- Grimbergen, J. L. T., Wapenaar, C. P. A., and Dessing, F. J., 1995, One-way operators in laterally varying media: 57th Conf., Eur. Assn. Geosci. Eng., Extended Abstracts, C032.
- Hale, D., 1991, Stable explicit depth extrapolation of seismic wavefields: Geophysics, **56**, 1770-1777.
- Holberg, O., 1988, Towards optimum one-way wave propagation: Geophys. Prosp., **36**, 99-114.
- Huang, L. J., and Wu, R. S., 1996, Prestack depth migration with acoustic screen propagators: 66th Ann. Internat. Mtg. Soc. Expl. Geophys., Expanded Abstracts, 415-418.
- Huang, L. J., and Fehler, M. C., 1997, Extended pseudo-screen migration with multiple reference velocities: 66th Ann. Internat. Mtg. Soc. Expl. Geophys., Expanded Abstracts, 1742-1745.
- Keys, R. G., 1985, Absorbing boundary conditions for acoustic media: Geophysics, **50**, 892-902.
- Margrave, G. F., 1998, Theory of nonstationary linear filtering in the Fourier domain with application to time variant filtering: Geophysics, **63**, 244-259.
- Robinson, E. A., and Silvia, M. T., 1981, Digital foundations of time series analysis: Wave equation space-time processing: Holden-Day.
- Saint Raymond, X., 1991, Elementary introduction to the theory of pseudodifferential operators: CRC Press.
- Stoffa, P. L., Fokkema, J. T., de Luna Freire, R. M., and Kessinger, W. P., 1990, Split-step Fourier migration: Geophysics, **55**, 410-421.
- Wapenaar, C. P. A., 1992, Wave equation based seismic processing: In which domain?: 54th Conf., Eur. Assn. Geosci. Eng., Extended Abstracts, B019.
- Wapenaar, C. P. A., and Dessing, F. J., 1995, Decomposition of one-way representations and one-way operators: 57th Conf., Eur. Assn. Geosci. Eng., Extended Abstracts, C031.
- Wu, R. S., 1994, Wide-angle elastic wave one-way propagation in heterogeneous media and an elastic wave complex-screen method: J. Geophys. Res., **99**, 751-766.

APPENDIX A
NOTATION

| Short | Full | Description |
|-------------------------------|--|---|
| Ψ | $\Psi(x, 0, \omega)$ | Space-domain wavefield at $z = 0$. |
| φ | $\varphi(k_x, 0, \omega)$ | Wavenumber domain wavefield at $z = 0$. |
| Ψ_{v_j} | $\Psi_{v_j}(x, \Delta z, \omega)$ | Space-domain wavefield at $z = \Delta z$, extrapolated with v_j . |
| φ_{v_j} | $\varphi_{v_j}(k_x, \Delta z, \omega)$ | Wavenumber domain wavefield at $z = \Delta z$, extrapolated with v_j . |
| $\Psi_{v(x)}$ | $\Psi_{v(x)}(x, \Delta z, \omega)$ | Space-domain wavefield at $z = \Delta z$, extrapolated with $v(x)$ using an unspecified algorithm. |
| $\varphi_{v(x)}$ | $\varphi_{v(x)}(k_x, \Delta z, \omega)$ | Wavenumber domain wavefield at $z = \Delta z$, extrapolated with $v(x)$ using an unspecified algorithm. |
| Ψ_{PSPI} | $\Psi_{\text{PSPI}}(x, \Delta z, \omega)$ | Space-domain wavefield at $z = \Delta z$, extrapolated with $v(x)$ using the PSPI algorithm. |
| φ_{PSPI} | $\varphi_{\text{PSPI}}(k_x, \Delta z, \omega)$ | Wavenumber domain wavefield at $z = \Delta z$, extrapolated with $v(x)$ using the PSPI algorithm. |
| Ψ_{NSPS} | $\Psi_{\text{NSPS}}(x, \Delta z, \omega)$ | Space-domain wavefield at $z = \Delta z$, extrapolated with $v(x)$ using the NSPS algorithm. |
| φ_{NSPS} | $\varphi_{\text{NSPS}}(k_x, \Delta z, \omega)$ | Wavenumber domain wavefield at $z = \Delta z$, extrapolated with $v(x)$ using the NSPS algorithm. |
| α_{v_j} | $\alpha_{v_j}(k_x, \omega)$ | Phase-shift extrapolator for constant velocity v_j . |
| $\alpha_{v(x)}$ | $\alpha_{v(x)}(k_x, x, \omega)$ | Phase-shift extrapolator for variable velocity $v(x)$. |
| A | $A(k_x, k'_x, \omega)$ | Full-Fourier domain phase-shift extrapolator for variable velocity $v(x)$. |
| β | $\beta(k_x, x, \omega)$ | Aperture compensation filter. |
| $\alpha_{v(x)}^{\text{aper}}$ | $\alpha_{v(x)}^{\text{aper}}(k_x, x, \omega)$ | Aperture-compensated phase-shift extrapolator for variable velocity $v(x)$. |
| k_{z_j} | $k_{z_j}(k_x, \omega)$ | Vertical wavenumber for constant velocity v_j . |
| $k_z(x)$ | $k_z(k_x, x, \omega)$ | Vertical wavenumber for variable velocity $v(x)$. |
| $\Psi _{v_j}$ | $\Psi _{v_j}(x, 0, \omega)$ | Space-domain wavefield at $z = 0$, windowed to be nonzero only where $v(x) = v_j$. |
| $\varphi _{v_j}$ | $\varphi _{v_j}(k_x, 0, \omega)$ | Wavenumber domain wavefield at $z = 0$, windowed to be nonzero only where $v(x) = v_j$. |
| $\Psi_{v_j v_j}$ | $\Psi_{v_j v_j}(x, \Delta z, \omega)$ | Space-domain wavefield at $z = \Delta z$, extrapolated with v_j , windowed to be nonzero only where $v(x) = v_j$. |
| Ω_j | $\Omega_j(x)$ | Windowing function which is unity where $v(x) = v_j$ and zero otherwise. |

APPENDIX B

FOURIER DOMAIN FORMULATION FOR PSPI

Equation (6) is repeated here as

$$\Psi_{\text{PSPI}}(x, \Delta z, \omega) = \int_{-\infty}^{\infty} \varphi(k_x, 0, \omega) \alpha(k_x, x, \omega) e^{ik_x x} dk_x. \quad (\text{B-1})$$

The Fourier transform of equation (B-1) along the x axis is

$$\varphi_{\text{PSPI}}(k'_x, \Delta z, \omega) = \frac{1}{2\pi} \int_{-\infty}^{\infty} \left[\int_{-\infty}^{\infty} \varphi(k_x, 0, \omega) \alpha(k_x, x, \omega) e^{ik_x x} dk_x \right] e^{-ik'_x x} dx. \quad (\text{B-2})$$

The variable k'_x is used to distinguish the wavenumbers of the Fourier transform step from those of the extrapolation process. Next, switch the order of integration (see Margrave, 1998, for a discussion):

$$\varphi_{\text{PSPI}}(k'_x, \Delta z, \omega) = \int_{-\infty}^{\infty} \varphi(k_x, 0, \omega)$$

$$\times \left[\frac{1}{2\pi} \int_{-\infty}^{\infty} \alpha(k_x, x, \omega) e^{ik_x x} e^{-ik'_x x} dx \right] dk_x. \quad (\text{B-3})$$

Then define

$$A(k_x, k'_x - k_x, \omega) = \frac{1}{2\pi} \int_{-\infty}^{\infty} \alpha(k_x, x, \omega) e^{-ix(k'_x - k_x)} dx, \quad (\text{B-4})$$

and substitute into equation (B-3)

$$\varphi_{\text{PSPI}}(k'_x, \Delta z, \omega) = \int_{-\infty}^{\infty} \varphi(k_x, 0, \omega) A(k_x, k'_x - k_x, \omega) dk_x. \quad (\text{B-5})$$

Rename the wavenumber variables so that equation (B-5) is the same form as equation (11):

$$\varphi_{\text{PSPI}}(k_x, \Delta z, \omega) = \int_{-\infty}^{\infty} \varphi(k'_x, 0, \omega) A(k'_x, k_x - k'_x, \omega) dk'_x. \quad (\text{B-6})$$

APPENDIX C
FOURIER DOMAIN FORMULATION FOR NSPS

Equation (9) is repeated here as

$$\varphi_{\text{NSPS}}(k_x, \Delta z, \omega) = \frac{1}{2\pi} \int_{-\infty}^{\infty} \Psi(x, 0, \omega) \alpha(k_x, x, \omega) e^{-ik_x x} dx. \quad (\text{C-1})$$

Replace $\Psi(x, 0, \omega)$ with its Fourier transform along the x axis:

$$\varphi_{\text{NSPS}}(k_x, \Delta z, \omega) = \frac{1}{2\pi} \times \int_{-\infty}^{\infty} \left[\int_{-\infty}^{\infty} \varphi(k'_x, 0, \omega) e^{ik'_x x} dk'_x \right] \alpha(k_x, x, \omega) e^{-ik_x x} dx. \quad (\text{C-2})$$

The variable k'_x is used to distinguish the wavenumbers of the Fourier transform of the input wavefield from those of the extrapolation process. The next step is to reverse the order of

integration (see Margrave, 1998, for a discussion):

$$\varphi_{\text{NSPS}}(k_x, \Delta z, \omega) = \frac{1}{2\pi} \int_{-\infty}^{\infty} \varphi(k'_x, 0, \omega) \times \left[\int_{-\infty}^{\infty} \alpha(k_x, x, \omega) e^{ik'_x x} e^{-ik_x x} dx \right] dk'_x. \quad (\text{C-3})$$

Then define

$$A(k_x, k_x - k'_x, \omega) = \frac{1}{2\pi} \int_{-\infty}^{\infty} \alpha(k_x, x, \omega) e^{-ix(k_x - k'_x)} dx, \quad (\text{C-4})$$

and substitute into equation (C-3)

$$\varphi_{\text{NSPS}}(k_x, \Delta z, \omega) = \int_{-\infty}^{\infty} \varphi(k'_x, 0, \omega) A(k_x, k_x - k'_x, \omega) dk'_x. \quad (\text{C-5})$$